

# Study of the one-neutron transfer reaction in $^{18}\text{O}$ + $^{76}\text{Se}$ collision at 275 MeV in the context of the NUMEN project

Irene Ciraldo<sup>1,2,\*</sup>, F. Cappuzzello<sup>1,2</sup>, M. Cavallaro<sup>1</sup>, D. Carbone<sup>1</sup>, S. Burrello<sup>3</sup>, A. Spatafora<sup>1,2</sup>, A. Gargano<sup>4</sup>, G. De Gregorio<sup>4,5</sup>, R. I. Magaña Vsevolodovna<sup>6</sup>, L. Acosta<sup>7</sup>, C. Agodi<sup>1</sup>, P. Amador-Valenzuela<sup>7</sup>, T. Borello-Lewin<sup>8</sup>, G. A. Brischetto<sup>1,2</sup>, S. Calabrese<sup>1,2</sup>, D. Calvo<sup>9</sup>, V. Capirossi<sup>9,10</sup>, E. R. Chávez Lomeli<sup>7</sup>, M. Colonna<sup>1,2</sup>, F. Delaunay<sup>1,2,11</sup>, H. Djapo<sup>12</sup>, C. Eke<sup>13</sup>, P. Finocchiaro<sup>1</sup>, S. Firat<sup>14</sup>, M. Fisichella<sup>1</sup>, A. Foti<sup>15</sup>, A. Hacisalihoglu<sup>16</sup>, F. Iazzi<sup>9,10</sup>, L. La Fauci<sup>1,2</sup>, R. Linares<sup>17</sup>, N. H. Medina<sup>8</sup>, M. Morales<sup>18</sup>, J. R. B. Oliveira<sup>8</sup>, A. Pakou<sup>19</sup>, L. Pandola<sup>1</sup>, H. Petrascu<sup>20</sup>, F. Pinna<sup>9,10</sup>, G. Russo<sup>2,15</sup>, E. Santopinto<sup>6</sup>, O. Sgouros<sup>1</sup>, M. A. Guazzelli<sup>21</sup>, S. O. Solakci<sup>14</sup>, V. Soukeras<sup>1,2</sup>, G. Souliotis<sup>22</sup>, D. Torresi<sup>1</sup>, S. Tudisco<sup>1</sup>, A. Yildirim<sup>14</sup>, V. A. B. Zagatto<sup>17</sup> for the NUMEN collaboration

<sup>1</sup>Istituto Nazionale di Fisica Nucleare, Laboratori Nazionali del Sud - Catania, IT

<sup>2</sup>Dipartimento di Fisica e Astronomia "Ettore Majorana", Università di Catania - Catania, IT

<sup>3</sup>Technische Universität Darmstadt, Fachbereich Physik, Institut für Kernphysik, Darmstadt, Germany

<sup>4</sup>INFN - Sezione di Napoli, Napoli, Italy

<sup>5</sup>Dipartimento di Matematica e Fisica, Università della Campania "Luigi Vanvitelli", Caserta, Italy

<sup>6</sup>INFN, Sezione di Genova, Genova, Italy

<sup>7</sup>Instituto de Física, Universidad Nacional Autónoma de Mexico - Mexico City, Mexico

<sup>8</sup>Instituto de Física, Universidade de São Paulo - São Paulo, Brazil

<sup>9</sup>Istituto Nazionale di Fisica Nucleare, Sezione di Torino, Italy

<sup>10</sup>DISAT, Politecnico di Torino, Italy

<sup>11</sup>LPC Caen, Normandie Université, ENSICAEN, UNICAEN, CNRS/IN2P3, Caen, France

<sup>12</sup>Ankara University, Institute of Accelerator Technologies, Turkey

<sup>13</sup>Department of Mathematics and Science Education, Faculty of Education, Akdeniz University, Antalya, Turkey

<sup>14</sup>Department of Physics, Akdeniz University - Antalya, Turkey

<sup>15</sup>Istituto Nazionale di Fisica Nucleare, Sezione di Catania, Italy

<sup>16</sup>Institute of Natural Sciences, Karadeniz Teknik University - Trabzon, Turkey

<sup>17</sup>Instituto de Física, Universidade Federal Fluminense - Niterói, Brazil

<sup>18</sup>Instituto de Pesquisas Energeticas e Nucleares IPEN/CNEN - São Paulo, Brazil

<sup>19</sup>Department of Physics and HINP, University of Ioannina - Ioannina, Greece

<sup>20</sup>IFIN-HH - Magurele, Romania

<sup>21</sup>Centro Universitario FEI - São Bernardo do Campo, Brazil

<sup>22</sup>Department of Chemistry and HINP, National and Kapodistrian University of Athens, Athens, Greece

E-mail: \*ciraldo@lns.infn.it



Content from this work may be used under the terms of the [Creative Commons Attribution 3.0 licence](#). Any further distribution of this work must maintain attribution to the author(s) and the title of the work, journal citation and DOI.

**Abstract.** Heavy-ion one-nucleon transfer reactions are promising tools to investigate single-particle configurations in nuclear states, with and without the excitation of the core degrees of freedom. An accurate determination of the spectroscopic amplitudes of these configurations is essential for the study of other direct reactions as well as beta-decays. In this context, the  $^{76}\text{Se}(^{18}\text{O}, ^{17}\text{O})^{77}\text{Se}$  one-neutron transfer reaction gives a quantitative access to the relevant single particle orbitals and core polarization transitions built on  $^{76}\text{Se}$ . This is particularly relevant, since it provides data-driven information to constrain nuclear structure models for the  $^{76}\text{Se}$  nucleus.

The excitation energy spectrum and the differential cross section angular distributions of this nucleon transfer reaction was measured at 275 MeV incident energy for the first time using the MAGNEX large acceptance magnetic spectrometer. The data are compared with calculations based on distorted wave Born approximation and coupled channel Born approximation adopting spectroscopic amplitudes for the projectile and target overlaps derived by large-scale shell model calculations and interacting boson-fermion model.

These reactions are studied in the frame of the NUMEN project. The NUMEN (NUclear Matrix Elements for Neutrinoless double beta decay) project was conceived at the Istituto Nazionale di Fisica Nucleare–Laboratori Nazionali del Sud (INFN-LNS) in Catania, Italy, aiming at accessing information about the nuclear matrix elements (NME) of neutrinoless double beta decay ( $0\nu\beta\beta$ ) through the study of the heavy-ion induced double charge exchange (DCE) reactions on various  $0\nu\beta\beta$  decay candidate targets. Among these, the  $^{76}\text{Se}$  nucleus is under investigation since it is the daughter nucleus of  $^{76}\text{Ge}$  in the  $0\nu\beta\beta$  decay process.

## 1. Introduction

The study of the one-neutron transfer reaction in  $^{18}\text{O} + ^{76}\text{Se}$  collision at 275 MeV is part of the NUMEN (NUclear Matrix Elements for Neutrinoless double beta decay) project [1, 2] at Laboratori Nazionali del Sud of Istituto Nazionale di Fisica Nucleare in Catania (INFN-LNS). NUMEN proposes an innovative experimental way for accessing information about nuclear matrix elements entering in the expression of neutrinoless double beta decay ( $0\nu\beta\beta$ ) rate from the double charge exchange reaction cross sections. These are nuclear processes presenting relevant analogies with  $0\nu\beta\beta$  decay [3–5], in which two neutrons decay in two protons emitting two electrons and no neutrinos. This process, if observed, will prove that neutrino and antineutrino are the same particle, as Majorana asserted [6].

### Studying

The  $^{76}\text{Ge}$  is one of the isotopes candidate for  $0\nu\beta\beta$  decay, having  $^{76}\text{Se}$  as daughter nucleus. Since the nuclear matrix elements corresponding to the  $^{76}\text{Se} \rightarrow ^{76}\text{Ge}$  and  $^{76}\text{Ge} \rightarrow ^{76}\text{Se}$  for transitions connecting the ground states are the same, studying these nuclear transitions is relevant for NUMEN purposes. The most interesting channel is DCE, however, all the other nuclear processes (elastic and inelastic scattering, single charge exchange, one- and two-nucleon transfer) are important sources of information, essential to build a constrained analysis of the nuclear states of interest for DCE and  $0\nu\beta\beta$ . The study of these reactions all together is made in a multi-channel approach to provide a good description of the complete network of nuclear reaction data both from the reaction and the structure calculation sides and in a full consistent way [7].

Recently, different nuclear structure and the reaction mechanisms have been successfully investigated thanks to heavy-ion transfer reactions [8–14]. A systematic study on heavy-ion-induced one- and two-neutron transfer reactions on different target nuclei was pursued at INFN-LNS by the  $(^{18}\text{O}, ^{17}\text{O})$  and  $(^{18}\text{O}, ^{16}\text{O})$  reactions at incident energies ranging from 84 to 275 MeV [8–12, 15–18]. MAGNEX large acceptance magnetic spectrometer [19–21] was used to detect the ejectiles.

Studying multi-nucleon transfer reaction channels is relevant for two reasons. Firstly, multi-nucleon transfer reactions are concurrent to double charge exchange ones. However, their

contribution to DCE cross section has been recently proved to be negligible for specific systems [22]. Secondly, nucleon transfer reactions are essential tools to investigate specific features of the nuclear structure.

In this context, the  $^{76}\text{Se}(^{18}\text{O}, ^{17}\text{O})^{77}\text{Se}$  reaction, presented for the first time in Ref. [23], tests the sensitivity of the one-nucleon transfer experimental cross section to different nuclear structure models. In addition, in order to constrain nuclear structure models for  $^{76}\text{Se}$  data-driven information are provided. In fact, relevant single particle orbitals and core polarization configurations built on  $^{76}\text{Se}$  are quantitatively accessible by a complete theoretical study of this reaction.

## 2. Experiment and data reduction

The experiment was carried out at INFN-LNS in Catania. The Superconducting Cyclotron provided a  $^{18}\text{O}^{8+}$  beam with 275 MeV incident energy. Then, it was sent to the MAGNEX scattering chamber where it impinged the  $^{76}\text{Se}$  target. This was produced by the INFN-LNS chemical laboratory and consists in a thin film of  $^{76}\text{Se}$  evaporated on a natural carbon backing.

The beam was stopped by a copper Faraday cup, that measured the integrated electric charge. The MAGNEX magnetic spectrometer [19] was used to analyze the reaction ejectiles and residual nuclei. The optical axis was centered at  $8^\circ$ , allowing to cover the range of scattering angles  $3^\circ < \theta_{lab} < 14^\circ$  thanks to the MAGNEX large angular acceptance. The focal plane detector [24] measured the vertical and horizontal positions and incident angles. The detected particle were identified and their trajectories reconstructed through specific techniques [25–32]. The excitation energy  $E_x$  and the Q-value were extracted by missing mass calculations based on momentum conservation and relativistic energy laws:  $E_x = Q_0 - Q$  (where  $Q_0$  is the ground-to-ground state reaction Q-value).

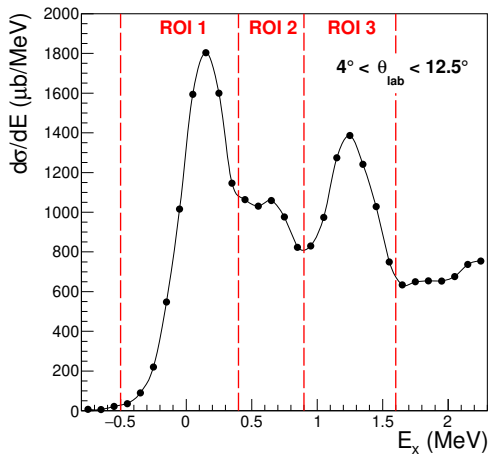


**Figure 1.**  $^{76}\text{Se}(^{18}\text{O}, ^{17}\text{O})^{77}\text{Se}$  differential cross section spectrum for  $4^\circ < \theta_{lab} < 12.5^\circ$  and  $-0.8 \text{ MeV} < E_x < 2.3 \text{ MeV}$ . To extract angular distributions three regions of interest (ROI) are selected by the dashed red lines.

Taking into account the overall MAGNEX efficiency [31], the technique described in Ref. [30] was used to extract the absolute cross sections. Fig. 1 shows the energy differential cross section spectrum for one-neutron stripping reaction. The error bars included in the spectrum indicate the statistical uncertainty, whereas, the one ( $\sim 10\%$ ) originated from the target thickness and the Faraday cup charge collection measurement is not indicated. The energy resolution is  $\delta E$  (FWHM)  $\sim 310$  keV and the angular resolution is  $\delta\theta_{LAB}$  (FWHM)  $\sim 0.5^\circ$ . Due to the high level density of the residual nucleus, single transitions were not resolved. Therefore, three regions of interest (ROI) are defined to extract the angular distributions corresponding to the superposition of different transitions:  $-0.5 < E_x < 0.4 \text{ MeV}$ ,  $0.4 < E_x < 0.9 \text{ MeV}$  and  $0.9 < E_x < 1.6 \text{ MeV}$ .

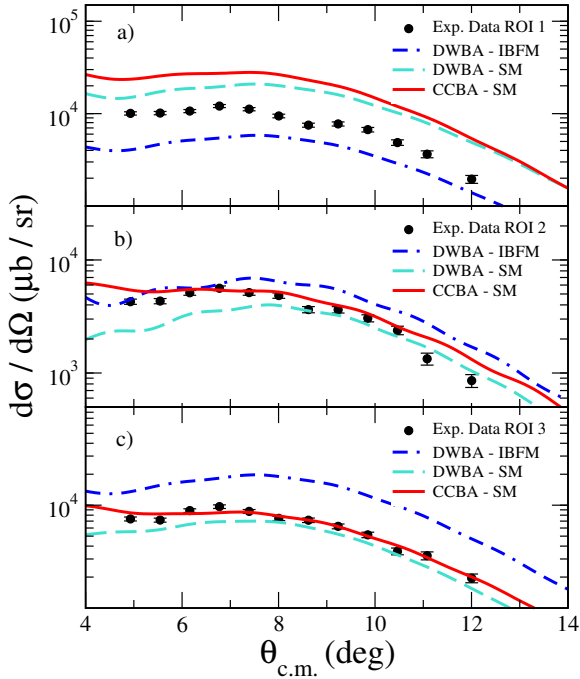


**Figure 2.** (color online) Comparison between theoretical and experimental cross sections for one-neutron transfer angular distributions related to the unresolved excited states of the three ROIs in Fig. 1. The DWBA (dashed cyan line), CCBA (continuous red line) calculations obtained using shell-model spectroscopic amplitudes (SM) are shown. DWBA (dotted-dashed blue line) calculations obtained using spectroscopic amplitudes from shell-model for the projectile and interacting boson-fermion model (IBFM) for the target are also plotted. (see text).

The experimental angular distributions, displayed in Fig. 2, are characterized by a sudden decrease for angles larger than  $\theta_{c.m.} \sim 9^\circ$ , corresponding to the grazing angle. The statistical error as well as the uncertainties coming from the solid angle and the efficiency correction are included in the error bars.

### 3. Theoretical analysis

The spectroscopic amplitudes for the projectile and target overlaps were calculated using to different nuclear structure models: Large Scale Shell-model (SM) and Interacting Boson model (IBM). Actually, the transfer matrix element and correspondingly the magnitude of the transfer cross section is determined essentially by the overlap of single-particle wave functions - obtained from a (self-consistent) mean-field calculation - with the initial and final nuclear states leading to the transfer form factors. For the reaction modeling Distorted Wave Born Approximation (DWBA) and Coupled Channel Born Approximation (CCBA) approaches are adopted.

#### 3.1. Shell model calculations

The KSHELL [33] code was used to derive the spectroscopic amplitudes for both projectiles and target within the shell model framework. The Zuker-Buck-McGrory (ZBM) effective interaction [34], already successfully used in many previous studies [8–11, 13, 18], was adopted for the projectile overlaps. The  $^{12}\text{C}$  is considered as a closed inert core and  $0p_{1/2}$ ,  $0d_{5/2}$ , and  $1s_{1/2}$  as valence orbits for both protons and neutrons. The psdmod [35] interaction, where the  $0d_{3/2}$  orbit is also accounted for, was recently adopted in Refs. [12, 17, 36] and allow to get good results also in this case.

For the target overlaps, the effective Hamiltonian was derived in the framework of many-body perturbation theory from the CD-Bonn nucleon-nucleon potential [37]. This last was renormalized using the  $V_{\text{low-}k}$  approach [38] with the addition of the Coulomb potential for protons. In particular, the  $\hat{Q}$ -box folded-diagram approach [39], including in the perturbative expansion of the  $\hat{Q}$ -box one and two-body diagrams up to the third order in the interaction, allowed to calculate the two-body matrix elements. This effective Hamiltonian was already

adopted in some recent studies [40, 41]. Moreover,  $^{56}\text{Ni}$  is considered as closed inert core and the model space for protons and neutrons is made up of four orbitals:  $0f_{5/2}$ ,  $1p_{3/2}$ ,  $1p_{1/2}$  and  $0g_{9/2}$ . The single-neutron and single-proton energies were taken from the experimental energy spectra of  $^{57}\text{Ni}$  [42] and  $^{57}\text{Cu}$  [42]. Since the energy of the proton for the  $0g_{9/2}$  orbital is not available, the neutron energy is adopted as well. The theoretical excitation energies of  $^{17}\text{O}$ ,  $^{18}\text{O}$ ,  $^{76}\text{Se}$  and  $^{77}\text{Se}$  states are reported in Ref. [23].

### 3.2. Interacting boson-fermion model

The interacting boson model (IBM-2) and neutron-proton interacting boson-fermion model (IBFM-2) were adopted to derive the spectroscopic amplitudes for target overlaps between  $^{76}\text{Se}$  and  $^{77}\text{Se}$  nuclei, respectively. These models were previously used in similar calculations [17, 18].

Even-even nuclei can be treated by IBM-2 replacing valence nucleon pairs with bosons having angular momentum 0 or 2 [43]. In particular, the  $^{76}\text{Se}$  nucleus was studied in Ref. [4, 44], where the model parameters are fitted to reproduce its energy levels [44], as reported in Ref. [23].

The IBM-2 formalism has been extended as IBFM-2 to study odd- $A$  nuclei by coupling an extra fermion to the boson system [45].  $^{77}\text{Se}$  is built by coupling one neutron to the core  $^{76}\text{Se}$ . The odd-fermion Hamiltonian [45, 46], the quasi-particle energy and the occupation probabilities of the odd particle are calculated in the Bardeen-Cooper-Schrieffer (BCS) approximation [47–51]. The required unperturbed neutron single-particle energies of the  $^{77}\text{Se}$  isotope were estimated by diagonalization of a Wood Saxon Potential. The same model space ( $0f_{5/2}$ ,  $1p_{3/2}$ ,  $1p_{1/2}$  and  $0g_{9/2}$ ) of the shell-model calculations was adopted. More details can be found in Ref. [23].

### 3.3. Reaction calculations

Cross section calculations were performed using the FRESCO code [52, 53] considering Distorted Wave Born Approximation (DWBA) and Coupled Channel Born approximation (CCBA) approaches.

The optical potentials for both the entrance and exit partitions were chosen according to the elastic and inelastic scattering analysis of the  $^{18}\text{O} + ^{76}\text{Se}$  collision at the same experimental conditions [54]. To describe the real and imaginary parts of the optical potential, the double-folding São Paulo potential was used. The same geometry and a different scaling factor are adopted. For DWBA calculations the scaling factor is 0.78 for both initial and final partition. For CCBA calculations, 0.6 is chosen as normalization coefficient to take into account all the channels not explicitly included in the system of coupled equations. The assumed scaling factors have been successfully used in the analyses of several scattering, charge exchange and transfer experimental data [8–10, 10–14, 17–19, 22, 36, 54–62].

For both the initial and final partitions couplings between the states are considered. As described in Ref. [54], the Coulomb and nuclear deformations for  $^{18}\text{O}$  and  $^{76}\text{Se}$  are obtained from experimental data [63], but they are compatible with those obtained from shell-model calculations. The signs of the reduced matrix elements  $M(E2)$ , defined in Refs. [14, 54, 55], are taken from shell-model calculations, according to the phase convention of the wave functions used to determine the spectroscopic amplitudes. Regarding the final partition, experimental data are often not available or not accurate. Therefore, the  $M(E2)$  and the corresponding deformation lengths, for the transitions characterized by the largest cross section, were calculated by shell model [23] to account for the couplings to inelastic states. Nevertheless, the effect on the calculated cross sections of the final partition couplings is found to be much smaller than the initial one.

The comparison between the theoretical and experimental angular distributions for the three ROIs of Fig. 1 is shown in Fig. 2. The DWBA and CCBA calculations obtained using shell-model spectroscopic amplitudes are plotted. The DWBA calculations obtained using

spectroscopic amplitudes from the interacting boson-fermion model for the target and shell-model for the projectile are also displayed. No arbitrary scaling factor is used in the calculations.

The slope of the curves is similar to the experimental data trend for DWBA and especially for the CCBA calculations. We found that CCBA calculations result in a slightly different diffraction pattern and a larger cross section respect to DWBA ones. In ROI 1 case, both DWBA and CCBA calculations slightly overestimate the experimental data. The inclusion of inelastic excitations of projectile and target improves the agreement between theory and experiment, resulting in a very good accord for ROIs 2 and 3.

In order to probe the cross section sensitivity to different nuclear structure theoretical models when the reaction mechanism is set, DWBA calculations using spectroscopic amplitudes from shell model for the projectile and from IBFM for the target were performed. Calculations using IBFM underestimate the experimental cross section in the ROI 1, whereas, they overestimate in the ROIs 2 and 3. The results are different from the shell-model ones, revealing that NUMEN experimental data are sensitive to different nuclear structure models.

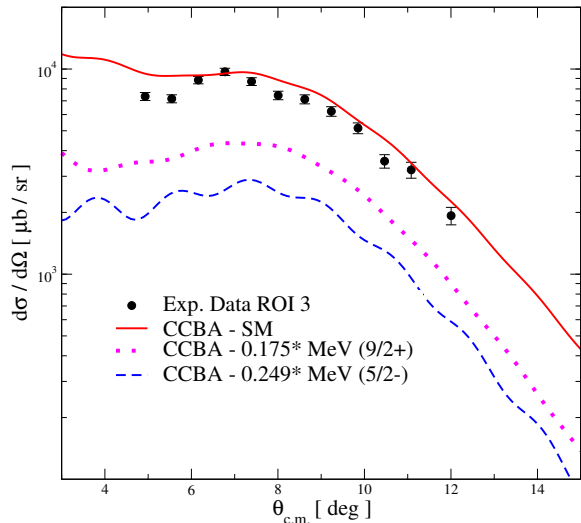


**Figure 3.** (color online) Comparison between the theoretical and experimental cross section for one-neutron transfer angular distribution related to the contribution of the unresolved excited states of the third ROI in Fig. 1. The transitions where the ejectile nucleus is found in its first excited state and the residual at 0.175 MeV (dashed blue line) and at 0.249 MeV (dotted magenta line) are shown together with the sum of all the contributing transitions for CCBA calculation (continuous red line).

Fig. 3 shows the angular distribution obtained integrating the third ROI of the differential cross section spectrum (Fig. 1) compared with CCBA calculations. In this region of the spectrum, the contribution of various excited states of the residual nucleus is expected. Despite the good experimental energy resolution, isolating the transitions which contribute more was not feasible from the experimental data only. On the contrary, thanks to the theoretical calculations it was possible to disentangle the strongest transitions. The strongest channels are the transitions where the ejectile nucleus is found in its first excited state ( $^{17}\text{O}_{0.870}(1/2^+)$ ) and the residual at 0.175 MeV and at 0.249 MeV. Other transitions contribute with orders of magnitude lower cross sections.

#### 4. Conclusions

In this manuscript, the study of the one-neutron transfer reaction in  $^{18}\text{O} + ^{76}\text{Se}$  collision at 275 MeV is presented. The experiment was carried out at the INFN-LNS laboratory in Catania in the context of the NUMEN project. Excitation energy spectra and differential cross section angular distributions were extracted. Due to the high level density for the residual nucleus, single transitions to  $^{77}\text{Se}$  and  $^{17}\text{O}$  were not resolved.

A comparison between experimental cross sections and theoretical calculations based on DWBA and CCBA approaches is performed. For the nuclear structure part, by shell-model and

interacting boson-fermion model are used to derive the one-neutron spectroscopic amplitudes for the projectile and target overlaps. The result is a remarkable agreement between theory and experiment, without using any arbitrary scaling factor. This proves that the adopted models for both the nuclear structure and the reaction mechanism account for the relevant processes occurring in the nuclear reaction studied. In addition, we found that the inclusion of inelastic excitations of projectile and target guarantees a better agreement. Moreover, thanks to the theoretical calculations it was possible to estimate the strongest transitions which contribute to the cross section of each ROI.

Calculations using IBFM underestimate the experimental cross section in the ROI 1, whereas, they overestimate in the ROIs 2 and 3. This result probes that the experimental data are sensitive to different nuclear structure models. This sensitivity is relevant for NUMEN purposes, indeed, it allows to find the more appropriate nuclear structure models to describe the nuclei involved in the DCE reactions. Therefore, the studies of heavy-ion multi-nucleon transfer reactions allow to benchmark nuclear structure models adopted to study other processes such as DCE reactions and even  $0\nu\beta\beta$  decay.

## 5. Acknowledgments

This project has received funding from the European Research Council (ERC) under the European Union's Horizon 2020 research and innovation programme (Grant Agreement No. 714625). We also acknowledge the CINECA award under the ISCRA initiative (code HP10B51E4M) and through the INFN-CINECA agreement for the availability of high performance computing resources and support.

## 6. References

- [1] Cappuzzello F, Agodi C, Cavallaro M *et al.* 2018 *Eur. Phys. J. A* **54** 72
- [2] Agodi C *et al.* 2021 *Universe* **7** 72
- [3] Cappuzzello F, Cavallaro M, Agodi C *et al.* 2015 *Eur. Phys. J. A* **51** 145
- [4] Santopinto E, García-Tecocoatzi H, na Vsevolodovna R I M and Ferretti J 2018 *Phys. Rev. C* **98** 061601
- [5] Lenske H, Cappuzzello F, Cavallaro M and Colonna M 2019 *Prog. Part. Nucl. Phys.* **109** 103716
- [6] Majorana E 1937 *Nuovo Cim.* **14** 171
- [7] Spatafora A *et al.* 2022 *Phys Rev. C* Submitted
- [8] Cavallaro M *et al.* 2013 *Phys. Rev. C* **88** 054601
- [9] Ermamatov M J *et al.* 2016 *Phys. Rev. C* **94** 024610
- [10] Carbone D *et al.* 2017 *Phys. Rev. C* **95** 034603
- [11] Linares R *et al.* 2018 *Phys. Rev. C* **98** 054615
- [12] Cardozo E N *et al.* 2018 *Phys. Rev. C* **97** 064611
- [13] Ferreira J L *et al.* 2021 *Phys. Rev. C* **103** 054604
- [14] Cavallaro M *et al.* 2021 *Front. Astron. Space Sci.* **8** 659815
- [15] Cappuzzello F, Carbone D, Cavallaro M, Bondì M, Agodi C, Azaiez F, Bonaccorso A, Cunsolo A, Fortunato L, Foti A *et al.* 2015 *Nature Commun.* **6** 6743
- [16] Cavallaro M, Cappuzzello F, Carbone D and Agodi C 2019 *Eur. Phys. J. A* **55** 244
- [17] Carbone D *et al.* 2020 *Phys. Rev. C* **102** 044606
- [18] Paes B, Santagati G, Vsevolodovna R M, Cappuzzello F, Carbone D, Cardozo E N, Cavallaro M, García-Tecocoatzi H, Gargano A, Ferreira J L, Lenzi S M, Linares R, Santopinto E, Vitturi A and Lubian J 2017 *Phys. Rev. C* **96** 044612
- [19] Cappuzzello F, Agodi C, Carbone D and Cavallaro M 2016 *Eur. Phys. J. A* **52** 169
- [20] Cappuzzello F, Carbone D, Cavallaro M and Cunsolo A 2011 *Magnets: Types, Uses and Safety* **52** 1–63
- [21] Cavallaro M *et al.* 2020 *Nucl. Inst. and Meth. B* **463** 334–338
- [22] Ferreira J L *et al.* 2022 *Phys. Rev. C* **105** 014630
- [23] Ciraldo I *et al.* 2022 *Phys Rev. C* **105** 044607
- [24] Torresi D *et al.* 2021 *Nucl. Inst. and Meth. A* **989**
- [25] Cappuzzello F *et al.* 2010 *Nucl. Inst. and Meth. A* **621** 419
- [26] Calabrese S *et al.* 2020 *Nucl. Inst. and Meth. A* **980** 164500
- [27] Souliotis G *et al.* 2022 *Nucl. Inst. and Meth. A* **1031** 166588
- [28] Cappuzzello F, Carbone D, and Cavallaro M 2011 *Nucl. Inst. and Meth. A* **638** 74

[29] Cappuzzello F, Agodi C, Bondì M, Carbone D, Cavallaro M, Cunsolo A, Napoli M D, Foti A and Nicolosi D 2014 *Nucl. Inst. and Meth. A* **763** 314

[30] Carbone D 2015 *Eur. Phys. J. Plus* **130** 143

[31] Cavallaro M, Cappuzzello F, Carbone D, Cunsolo A, Foti A and Linares R 2011 *Nucl. Inst. and Meth. A* **637** 77

[32] Ciraldo I 2021 *Nuovo Cim.* **44 C** 38

[33] Shimizu N, Mizusaki T, Utsuno T and Tsunoda Y 2019 *Comput. Phys. Commun.* **244** 372

[34] Zuker A P, Buck B and McGrory J B 1968 *Phys. Rev. Lett.* **21** 39

[35] Utsuno Y and Chiba S 2011 *Phys. Rev. C* **83** 021301

[36] Sgouros O *et al.* 2021 *Phys. Rev. C* **104** 034617

[37] Machleidt R 2001 *Phys. Rev. C* **63** 024001

[38] Bogner S, Kuo T T S and Coraggio L 2001 *Nucl. Phys. A* **684** 432c

[39] Coraggio L, Covello A, Gargano A *et al.* 2012 *Ann. Phys.* **327** 2125

[40] Coraggio L *et al.* 2019 *Phys. Rev. C* **100** 014316

[41] Rocchini M *et al.* 2021 *Phys. Rev. C* **103** 014311

[42] *Data extracted using the NNDC On-Line Data Service from the ENSDF database* (<http://www.nndc.bnl.gov/ensdf/>)

[43] Iachello F and Arima A 1984 *Adv. Nucl. Phys.* 139–200

[44] Kaup U, Mönkemeyer C and v Brentano P 1983 *Z. Phys. A* **310** 129

[45] Iachello F and Isacker P V 1991 *The Interacting Boson-Fermion Model* Cambridge Monographs on Mathematical Physics (Cambridge University Press) doi:10.1017/CBO9780511549724

[46] Ferretti J, Kotila J, Vsevolodovna R I M and Santopinto E 2020 *Phys. Rev. C* **102** 054329

[47] Bardeen J, Cooper L N and Schrieffer J R 1957 *Phys. Rev.* **108** 1175

[48] Alonso C E, Arias J M, Bijker R and Iachello F 1984 *Phys. Lett.* **144B** 141

[49] Arias J M 1985 PhD dissertation University of Sevilla

[50] Alonso C E 1986 PhD dissertation University of Sevilla

[51] Aria J M, Alonso C E and Bijker R 1985 *Nucl. Phys. A* **445** 333

[52] Thompson I J 1988 *Phys. Rep.* **7** 167

[53] Thompson I and Nunes F 2009 *Nuclear Reactions for Astrophysics: Principles, Calculation and Applications of Low-Energy Reactions*, 1st ed. (Cambridge University Press, Cambridge, U.K.)

[54] Fauci L L, Spatafora A *et al.* 2021 *Phys. Rev. C* **104** 054610

[55] Carbone D *et al.* 2021 *Universe* **7** 58

[56] Spatafora A *et al.* 2019 *Phys Rev. C* **100** 0346206

[57] Zagatto V *et al.* 2018 *Phys. Rev. C* **97** 054608

[58] Oliveira J R B *et al.* 2013 *J. Phys. G: Nucl. Part. Phys.* **40** 105101

[59] Pereira D *et al.* 2012 *Phys. Lett. B* **710** 426

[60] Ermamatov M J *et al.* 2017 *Phys. Rev. C* **96.4** 044603

[61] Burrello S, Calabrese S *et al.* 2022 *Phys. Rev. C* **105** 024616

[62] Calabrese S *et al.* 2021 *Phys. Rev. C* **104** 064609

[63] Pritychenko B, Birch M, Singh B and Horoi M 2016 *Data Nucl. Data Tables* **107** 1